Archives of Hydro-Engineering and Environmental Mechanics
Vol. 50 (2003), No. 1, pp. 59–72

Local Cavitation Due to Water Hammer

Marek Mitosek*, Apoloniusz Kodura*, Elżbieta Rybak-Wilusz**

*Warsaw University of Technology, Institute of Water Supply and Water Engineering,
Nowowiejska 20, 00–653 Warsaw, Poland, e-mail: Marek.Mitosek@is.pw.edu.pl,
Apoloniusz.Kodura@is.pw.edu.pl

**Rzeszów Technical University, Department of Building and Environmental Engineering,
Al. Powstańców Warszawy 6, 35–329 Rzeszów, Poland, e-mail: elrywi@prz.rzeszow.pl

(Received March 08, 2003; revised June 10, 2003)

Abstract

The phenomenon of vapour cavitation due to water hammer is investigated experimentally using high frequency pressure transducers (piezoelectric and strain gauges). The water hammer is caused by a sudden closure of a ball valve mounted at the end of the steel pipe. A short-duration pressure pulse, as well as high frequency cavitation pressure oscillations are observed. The high frequency pressure oscillations appear just after the vapour cavity collapse, whereas the pressure pulse does not occur immediately after collapse but is delayed from 0 to the water hammer period $2L/c$. The experiments have shown that the maximum high frequency pressure oscillation, directly proportional to the pressure wave velocity, can be many times higher than the maximum water hammer pressure amplitude as well as short-duration pressure pulse. The influence of liquid evaporation duration and the steady state losses on the maximum high frequency cavitation pressure oscillation are shown. Growing pressure reduction is accompanied by gas desorption from the liquid. The liberated air reduces the amplitude of the pressure increase and prolongs the period of oscillations. The experiments have shown that there are three phases of the maximum amplitude of high frequency pressure oscillations for each fixed steady state loss. The frequency of vapour cavitation pressure oscillations depends on the duration of the oscillations. For the test cases, the frequency increases during the cavitation from ca. 400 to 900 Hz for steel pipes.

Keywords: water hammer, cavitation, pressure oscillations, gas desorption

Notations

c – pressure wave velocity,
D – inside diameter of a pipe,
e – pipe wall thickness,
L – pipe length,
p – pressure,

p_0 – pressure at the outlet valve,
p_s – water pressure at the inlet to the installation,
t – time,
t_v – evaporation time,
t_z – valve closure time,
T – period of water hammer,
T_c – period of local cavitation oscillation,
v_0 – velocity of steady flow,
Δp – water hammer pressure rise (first amplitude),
Δp_c – maximum cavitation pressure rise,
Δv – change in velocity,
ρ – liquid density.

1. Introduction

Transient cavitation frequently occurs in liquid-filled pipe-lines in unsteady flow conditions. The phenomenon is one of the additional phenomenon accompanying the water hammer. It is a local formation which develops whenever the fluid pressure drops below a certain critical value, approximating to vaporization pressure of the fluid. Cavitation is the nucleation, growth and collapse or gradual diminution of bubbles. The vapour bubbles generated at vapour pressure are accompanied by air liberated due to desorption. For cavitation which lasts longer than 1.5 s, Zielke et al. (1989) find that gas release effect should be taken into account. However, experiments carried out later show that this influence is also observed for very short duration of vapour pressure (Mitosek 1997).

There are two theories to explain the cavitation damage (Shima 1997). One concerns the impulsive pressures or shock waves caused by the collapse of bubbles, and the other – the microjet which was induced from the non-spherical collapse of the bubbles. The influence of pressure increase due to cavitation and pressure oscillation caused by water hammer can be harmful to the pipe wall and its fatigue life.

In fully-filled piping systems transient cavitation is normally characterised by two flow regimes: a distributed cavitation and a column separation. In the distributed cavitation region (two phase flow) vapour bubbles are dispersed in the liquid. In the column separation region, the bubble population is sufficiently large to coalesce to form a vapour pocket. With a pipeline of varying elevation the vapour pocket usually forms near one of the high points in the profile. Discrete vapour-cavity DVCM models and discrete gas-cavity DGCM model are used to describe the column separation (Kronenburg 1974, Kot and Youndahl 1978, Wylie and Streeter 1993).

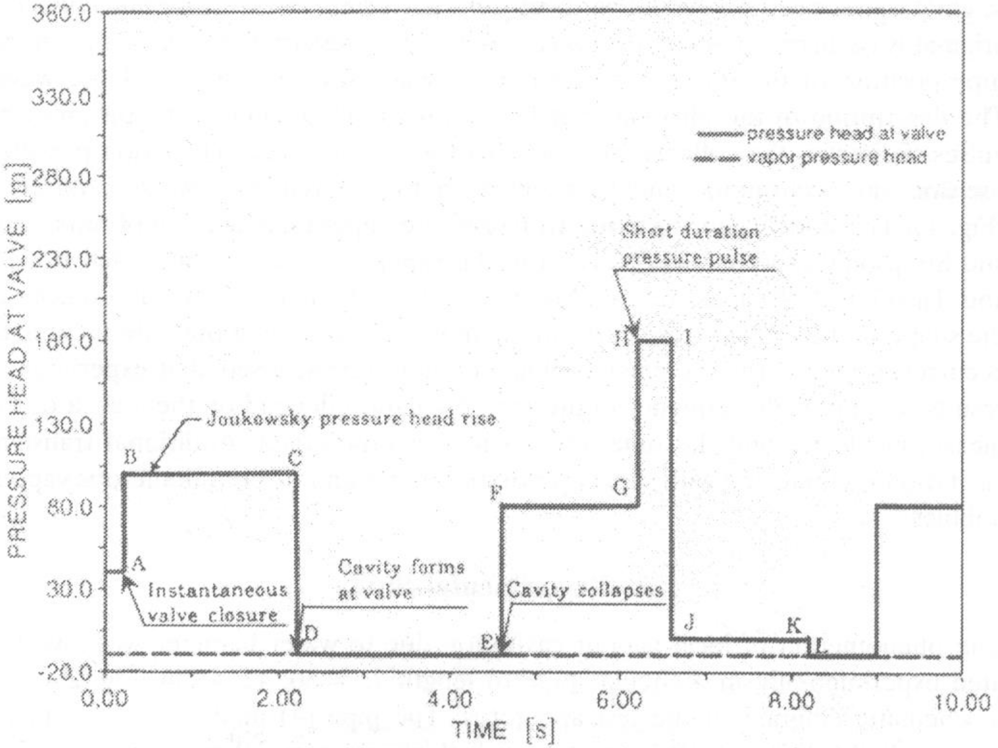

Fig. 1. Superposition of the collapsed cavity pressure head and water hammer head (Simpson and Wylie 1991)

During the cavitation due to water hammer the maximum pressure increase may exceed the Joukowsky pressure rise as computed from $\Delta p = -\rho \cdot c \cdot \Delta v$, where: ρ – stream density, Δv – difference in final and initial stream velocities and c – wave velocity (Simpson and Wylie 1991). Large pressure resulting from the collapse of vapour cavity is referred to as a short-duration pressure pulse. The maximum pressure occurs as a narrow short-duration pressure pulse, resulting from the superposition of the collapsed cavity pressure and the water hammer – Fig. 1 (Simpson and Wylie 1991). The pressure generated by the cavity collapse is less then the water hammer pressure increase. An explanation of the physical formation of a short-duration pressure pulse for a simple reservoir-valve system connected by a pipe is as follows. Upon instantaneous valve closure (A-B in Fig. 1), a pressure wave passes from the valve towards the reservoir. The wave reflects from the reservoir and travels back to the valve, arriving at the valve at $2L/c$ after closure, where L is pipe length. The pressure at the valve then drops below the initial steady state to a vapour pressure (C-D). A cavity forms at (D) and collapses at (E). The time of existence of the cavity is equal to the distance (D-E). When the cavity collapses a pressure rise occurs (E-F). The sudden cavity collapse has produced a second water hammer wave in the pipe in addition to the original valve closure wave. The short-duration pressure pulse occurs when the original wave arrives back at the valve (G-H). The pressure pulse results from the superposition of the initial (water hammer) wave and the cavity collapse wave. The description of the physical formation shows that for short-duration pressure pulses, following the collapse of vapour cavity, the maximum cavitation pressure rise does not occur immediately on collapse but is delayed by between 0 and $2L/c$ (Fig. 1). This conclusion, resulting from discrete vapour-cavity model simulations and Simpson's experiment, differs from the experiment results published by Fan and Tijsseling (1992), as well as, Mitosek (1997, 2000). There are differences in the shape of the pressure rise curve in the moments of the first pressure increment occurrence and in the increment values. It should be stressed that experimental results for very high frequency of pressure oscillation depend on the inertia of the measuring device and the time interval for recording data. Additional transient cavitation is connected with short evaporation times and tiny but numerous vapour bubbles.

2. Experimental Study

The phenomenon of local vapour cavitation due to water hammer was investigated experimentally in a circular pipe of length L = 30, 42, 48 m. Fig. 2 shows a schematic diagram of the test apparatus. The pipe (4) made of steel with inside diameter D = 42 ±0.1 mm and wall thickness e = 3.0 mm was used. The phenomenon was caused by a water hammer resulting from a sudden closure of a ball valve (5) mounted at the end of the pipe. The measurement and analysis of pressure characteristics $p(t)$ referred to simple water hammer in which the pressure wave period T was always greater than the valve closure time t_z (t_z = 0.025 ÷ 0.030 s).

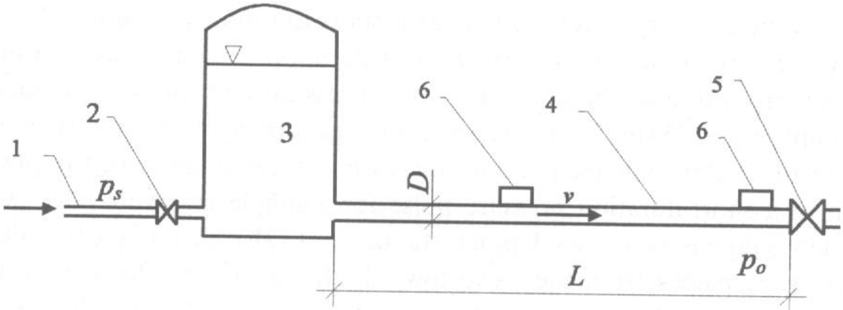

Fig. 2. Measuring stand: 1 – supply pipe, 2 – pressure reducing valve, 3 – reservoir, 4 – pipe, 5 – ball valve, 6 – strain gauge

Pressure wave velocities c, where $c = 2L/T$, calculated for a measured period of water hammer, at a temperature of 283±2K, amounted to $c \approx 1260 \div 1280$ m/s. Pressure characteristics $p(t)$ at two points of the pipe-line were measured.

The points were located at the valve mounted at the end and in the middle part of the pipe (6). Pressure was recorded by means of a measuring system consisting of strain gauges and piezoelectric gauges, extensometer amplifier and computer with AD/DA card. The pressures were recorded at intervals of the order of 10^{-5}s. The strain gauges were selected according to the expected maximum pressure at measuring points in the pipe and were fastened onto the pipes in the manner shown in Fig. 3. The piezoelectric gauge was in direct contact with the water stream (b) or connected with the stream by a short, small pipe (c).

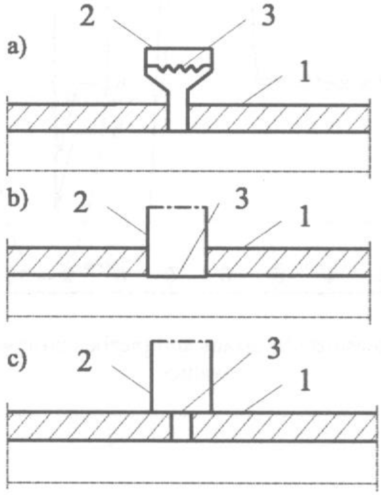

Fig. 3. Fastening of gauges to the pipe:
a) strain gauge, b) piezoelectric gauge without pipe stub, c) piezoelectric gauge with pipe stub,
1 – pipe, 2 – sensor, 3 – pressure impulses measuring area

The tested pipe (Fig. 1) was fed from a large pressure reservoir (3) supplied from a water pipe network. The water pressure p_s at the inlet to the installation was constant($p_s = 0.65 \pm 0.01$ MPa) and was reduced just at the reservoir by a valve (2). By reducing the pressure p_s and applying different water flow velocities v the stream pressure value p_o at the outlet was changed. The steady-state velocity v varied from 0.5 to 2 m/s allowing different pressures p_o and various pressure amplitudes Δp for the first positive wave to be obtained. The evaporation time t_v, caused by a decrease in pressure to the vapour pressure p_v at a given stream temperature, was also variable.

3. Local Cavitation

In Figures 4, 5, 6 and 7 the recorded characteristics $p(t)$ at terminal valve for steel pipe measured by piezoelectric gauge and strain gauge are presented.

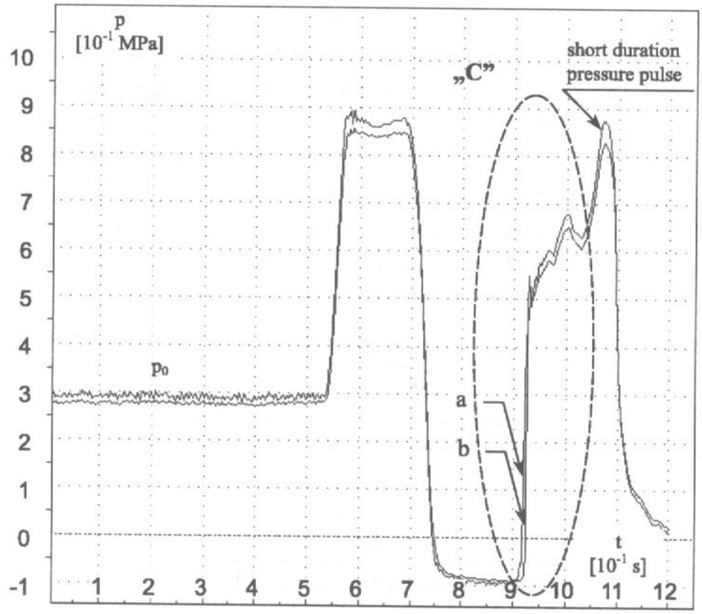

Fig. 4. Characteristic $p(t)$ measured by strain and piezoelectric gauges – averaged measuring values

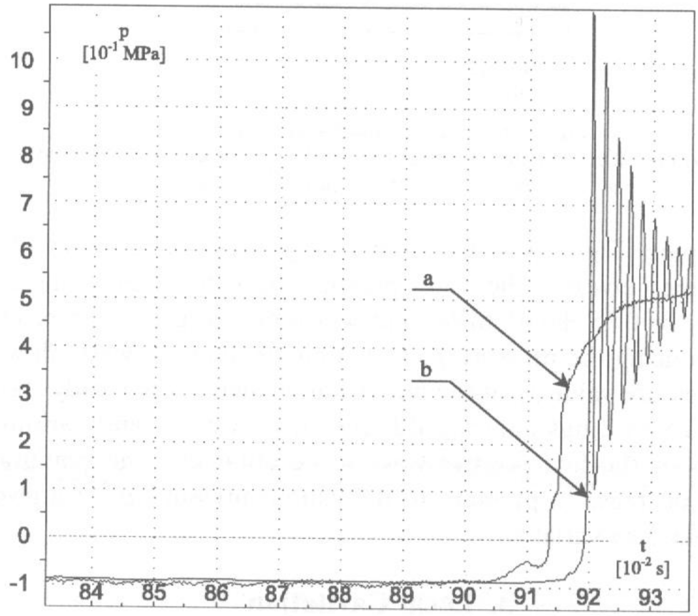

Fig. 5. Detail "C" of $p(t)$ shown in Fig. 4; a) piezoelectric gauge measurement without connecting pipe, b) strain gauge measurement

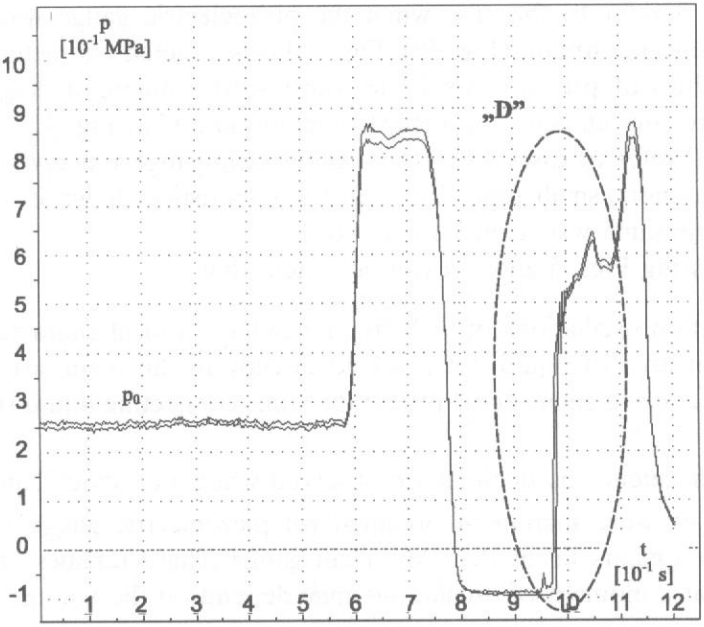

Fig. 6. Characteristic $p(t)$ measured by strain and piezoelectric gauges – averaged measuring values

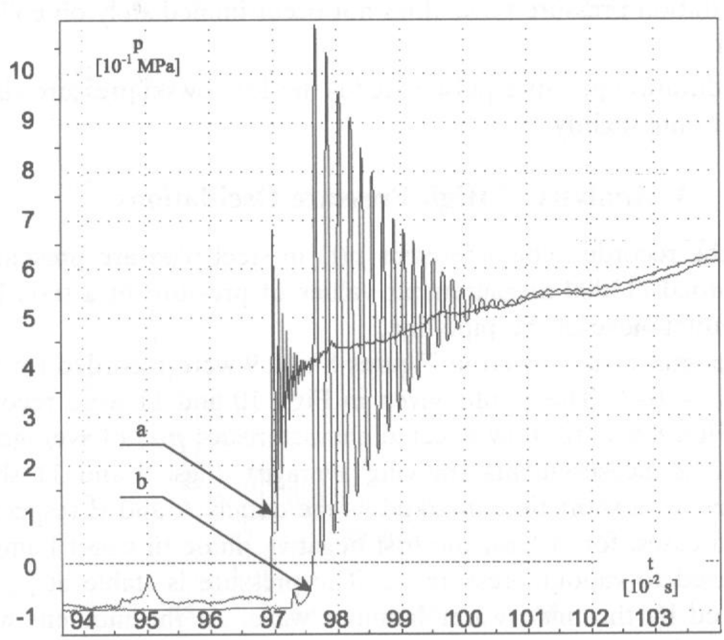

Fig. 7. Detail "D" of $p(t)$ shown in Fig. 6; a) piezoelectric gauge measurement with connecting pipe, b) strain gauge measurement

Figs. 4 and 5 refer to the case when the piezoelectric gauge was in direct contact with the water stream (Fig. 3b). Fig. 4 shows selected characteristics $p(t)$ of averaged values of pressure for 12 measurements (moving average). Fig. 5 presents real pressure changes for a short time, marked C in Fig. 4.

Figs. 6 and 7 refer to cases when the piezoelectric gauge was connected with the stream by a short, small pipe (Fig. 3c). Characteristics shown in the figures were made in the same way as in Figs. 4 and 5.

After comparing Figs. 5 and 7 it can be stated, that:

- the cavitation oscillations of high frequency have a local character and appear in an area of liquid not involved directly in the main stream – in a dead space, e.g. a small, short pipe (pipe stub) connecting liquid stream and a gauge,
- the high frequency oscillations are observed when a cavity collapses,
- observed pressure increment obtained for piezoelectric gauge (characteristics "a") appears faster than for strain gauge (characteristics "b"), which means that a moment of oscillations may depend on the volume of a dead zone,
- cavitation oscillations of high frequency fluctuate about the main wave of water hammer,
- a short duration pressure pulse does not occur immediately on collapse but is delayed,
- the short duration pressure pulse exceeds the Joukowski pressure rise rather rarely and only slightly.

4. Analysis of High Pressure Oscillations

In Figs. 8–11, the recorded characteristics $p(t)$ in steel pipe are presented. The curves are recorded (15000 measurement values of pressure in a test) by strain gauges at the outlet valve of the pipe-line.

The experimental results given in Figures 8 and 9 were recorded for pressure reduction $p_o/p_s = 0.46$. The results given in Figs. 10 and 11 were recorded for $p_o/p_s = 0.31$. Figs. 8 and 10 show selected characteristics $p(t)$ of averaged values of pressure for 12 measurements (moving average). Figs. 9 and 11 show real pressure changes for a short time, marked as the details A and B respectively.

In presented cases, for at least the first negative phase of water hammer, the pressure decreased to vapour pressure p_v. The pressure is stable at p_v until its increase is forced by the main water hammer wave. At the moment when the pressure increase begins, rapid collapse of bubbles causes a vapour cavitation phenomenon – that is, an additional, rapidly changing, set at damped pressure oscillations appear.

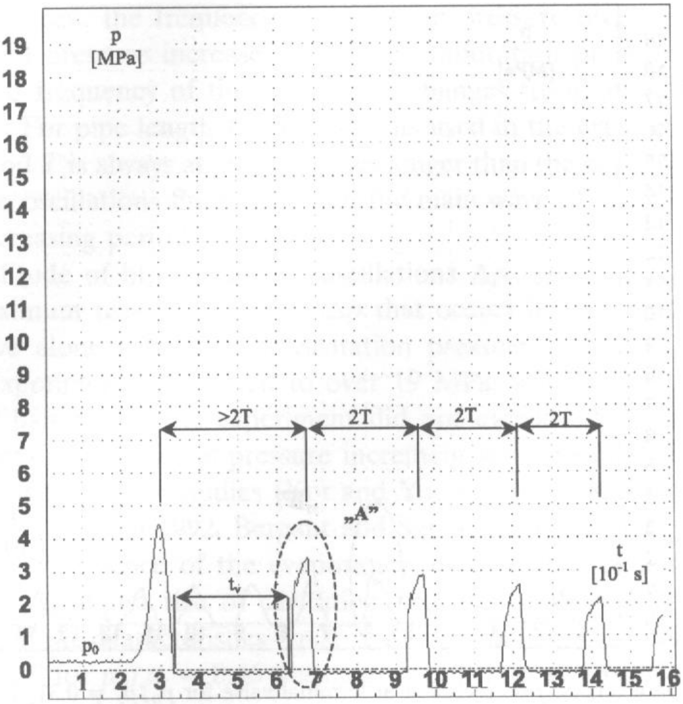

Fig. 8. Characteristic $p(t)$ recorded at exhaust valve for $p_o/p_s = 0.46$, $T = 283$K

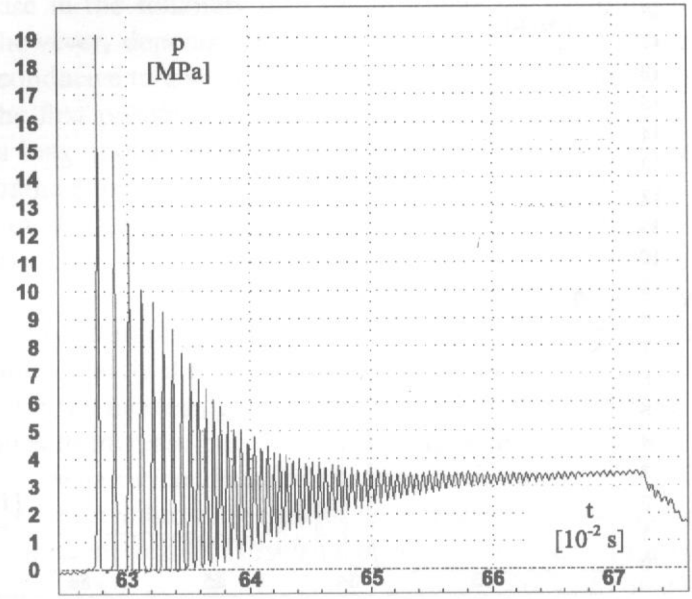

Fig. 9. Detail "A" – pressure values without averaging at end of first negative phase of water hammer

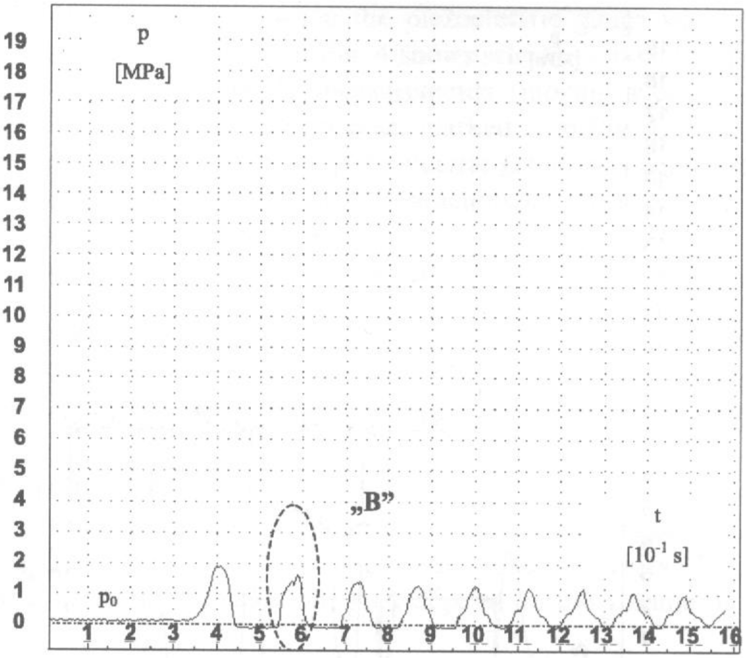

Fig. 10. Characteristic $p(t)$ recorded at terminal valve for $p_o/p_s = 0.31$, $T = 283$K

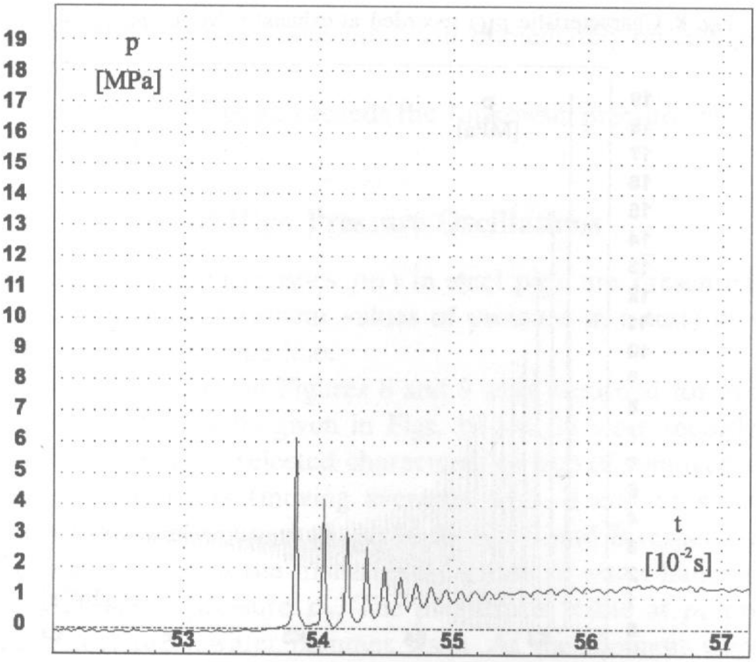

Fig. 11. Detail "B" – pressure values without averaging at end of first negative phase of water hammer

As can be seen, the frequency of cavitation pressure oscillations during the initial phase of pressure increase above the evaporation pressure p_v, increases. The measured frequency of the oscillations changes from about 400 to 900 Hz for steel pipe. For pipe length L and materials used in the experiments, the water hammer period T is always at least 20 times longer than the cavitation wave period T_c. Cavitation oscillations fluctuate about the main wave of water hammer with a gradually decreasing period T_c.

The amplitude of high frequency oscillations Δp_c can be many times higher than the maximum pressure increase Δp that occurs for the first positive water hammer wave alone. The highest cavitation pressure increment Δp_c recorded during the experiments amounted to over 19 MPa, whereas the first amplitude Δp of water hammer in the experiment did not exceed 5.5 MPa for steel pipe used. The measured values of pressure increment were distinctly higher than the results published in other studies (Kot and Youndahal 1978, Simpson and Wylie 1991, Fan and Tijsseling 1992, Bergant and Simpson 1999).

The distinct influence of the evaporation time t_v and reduction of pressure p_o/p_s on the maximum rise of cavitation pressure oscillation Δp_s is shown in Fig. 12. Each of the characteristics $\Delta p_c(t_v)$: curve 1 for pressure reduction $p_o/p_s = 0.31$ and curve 2 for $p_o/p_s = 0.46$ was determined from at least 25 measurements.

The pressure reduction p_o/p_s in steady flow decreases the cavitation pressure increments. The pressure reduction may cause supersaturation through an associated decrease in the solubility of a gas in a liquid – according to Henry's law. Desorption however, depends greatly upon the duration of the instability. Gas evolution is conducive to a weakening of the pressure wave at water hammer, e.g. diminishes the first positive pressure increment. It is important that the time of desorption is long enough, so that the created gas bubbles are sufficiently large and do not immediately collapse with increasing pressure.

Analysis of the characteristics $\Delta p_c(t_v)$ has shown that three phases of the maximum amplitude of cavitation pressure oscillation for constant pressure reduction $p_o/p_s =$ const. can be distinguished there. At the beginning, for the short liquid evaporation duration, the value of the maximum pressure amplitude fast increases, approximately directly proportional to the evaporation duration – first phase. Then, for the increasing evaporation duration the maximum pressure amplitude continues to increase but this is slower than in the previous, second phase. For the longer evaporation duration the maximum pressure amplitude becomes stabilised, a constant value of the pressure is reached – third phase.

The measurement results (first and third phases) were approximated with a linear dependence $\Delta p_c = At_v + B$. The calculated values of equation parameters A and B as well as determination coefficients R^2 and standard errors S_e are given in Table 1. Characteristic evaporation time t_v recorded at each series of the measurements ($p_o/p_s =$ const.) is also given in Table 1. The second phase presented in Fig. 12 is a transient phase.

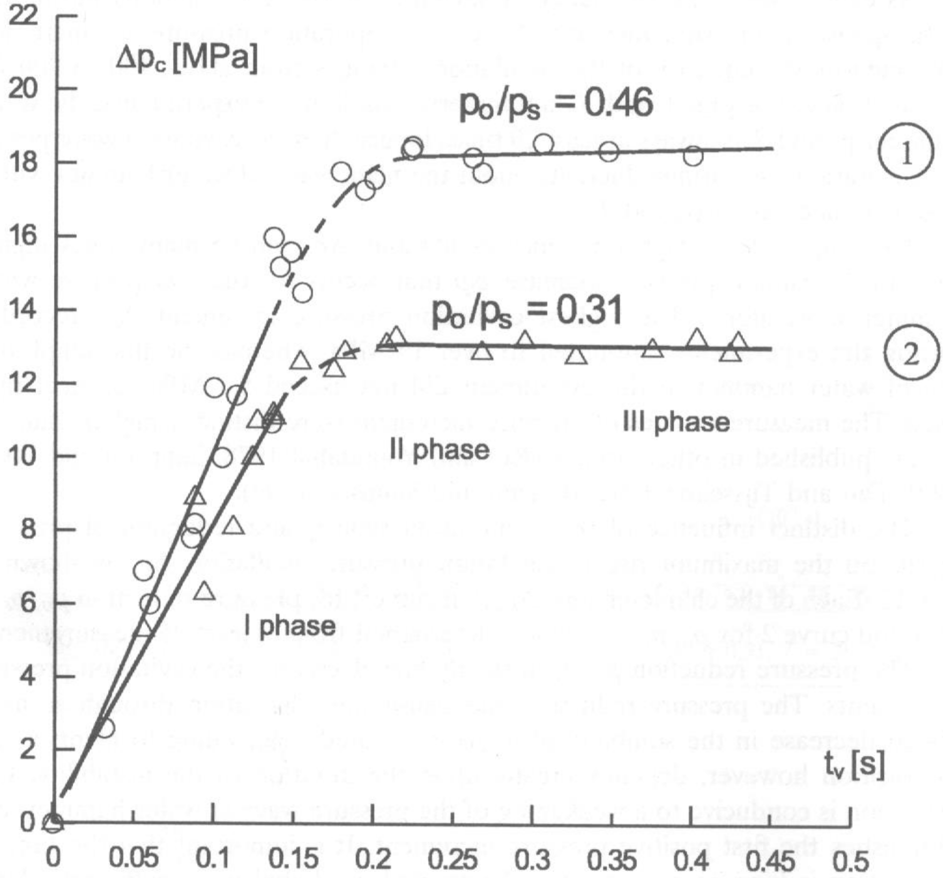

Fig. 12. Maximum cavitation pressure increase for steel pipe as function of evaporation duration $\Delta p_c(t_v)$ for two values of pressure reduction p_o/p_s

Table 1. Coefficients A and B, determination coefficients R^2 and standard errors S_e for curves shown in Fig. 12 for first (I) and third (III) phases (Rybak-Wilusz 2001)

Phase	I		III	
Curve number	1	2	1	2
p_o/p_s [–]	0.31	0.46	0.31	0.46
A [MPa/s]	79.012	102.88	−0.226	1.267
B [MPa]	0.311	−0.094	13.152	17.943
R^2 [–]	0.931	0.946	0.008	0.035
S_e [MPa]	0.172	0.178	0.160	0.110
range of t_v [s]	to 0.149 (max)	to 0.136 (max)	0.214 ÷ 0.429	0.223 ÷ 0.400

As can be seen, in the first phase the cavitation pressure oscillation increment Δp_c is caused by increased evaporation time t_v. If the evaporation time increases continuously, the part of vapour bubbles grows and gradually diminish when the pressure increases. The third phase is connected with relativity big free gas contents (air and vapour) in water, which decreases wave velocity and at the same time stabilises Δp_c. Finally, it can also be expected that the cavitation oscillation increment Δp_c will decrease for further increase in time t_v.

5. Conclusions

1. Local cavitation in the pipe due to water hammer contains two phenomena: damped high frequency pressure oscillations and a short-duration pressure pulse. However, the high frequency pressure oscillations appear in an area of liquid not involved directly in the main stream (in a dead space of liquid stream).
2. The frequency of pressure oscillations in steel pipes increases during the cavitation from ca. 400 to 900 Hz. Values of maximum pressure oscillation Δp_c may be many times higher than the maximum pressure amplitude of water hammer, as well as the short-duration pressure pulse.
3. The maximum increase in cavitation oscillation pressure Δp_c depends on the evaporation time t_v of the liquid and the degree of pressure reduction p_o/p_s in a stream at steady flow. The maximum pressure Δp_c decreases with stream pressure reduction p_o/p_s. A growing pressure reduction is accompanied by gas desorption from the liquid. The liberated air reduces the amplitude of the pressure increase and prolongs the period of oscillations.
4. Three phases of maximum amplitude of cavitation pressure Δp_c may be distinguished for increasing evaporation time t_v. The first phase – pressure increase, the second – transient phase and the third phase – pressure stabilisation. The stabilisation phase is connected with relatively big free gas contents in the stream.
5. The pressure oscillation of local cavitation in the pipe due to water hammer may be many times higher than the short duration pressure pulse in liquid stream. The local cavitation could be the main reason for the cavitation corrosion.

References

Bergant A., Simpson A. R. (1999), Pipeline Column Separation Flow Regimes, *Journal of Hydraulic Engineering,* 125 (8), 835–848.

Fan D., Tijsseling A. (1992), Fluid Structure Interaction with Cavitation in Transient Pipe Flows, *ASME Journal of Fluids Engineering,* 114 (6), 268–274.

Kot C. D., Youndahl C. K. (1978), Transient Cavitating Effects in Fluid Piping Systems, *Nuclear Engrg. and Des.* 45(1), 93–100.

Kronenburg C. (1974), Gas Release during Transient Cavitation in Pipes, *Journal of Fluids Div. ASCE*, 100 (10), 1383–1398.

Mitosek M. (1997), Study of Cavitation due to Water Hammer in Plastics Pipes, *Plastics, Rubber and Composites Processing and Applications*, 26 (7), 324–329.

Mitosek M. (2000), Study of Transient Vapor Cavitation in Series Pipe Systems. *Journal of Hydraulic Engineering ASCE*, 126 (12), 904–911.

Rybak-Wilusz E. (2001), *The Cavitation Phenomenon in Pipes in Unsteady Flow of Water*, PhD Thesis, Warsaw University of Technology (in Polish).

Simpson A. R., Wylie E. B. (1991), Large Water Hammer Pressures for Column Separation in Pipelines, *Journal of Hydraulic Engineering ASCE*, 117 (10), 1310–1316.

Simpson A. R., Bergant A. (1994), Numerical Comparison of Pipe Column Separation Models, *Journal of Hydraulic Engineering ASCE*, 120 (3), 361–377.

Shima A. (1997), *Studies on Bubble Dynamics*, Shock Waves, Springer Verlag 7, 33–42.

Wylie E. B., Streeter V. L., Suo L. (1993), *Fluid Transients in Systems*, Prentice-Hall, Inc., Upper Saddle River, New York.

Zielke W., Perko H. D., Keller A. (1989), Gas Release in Transient Pipe Flow, *Proc. 6th Int. Conf. on Pressure Surges BHRA*, Cranfield U.K., 3–13.